CellPress

Chemistry & Biology
Article

Identification of CDP-Archaeol Synthase, a Missing Link of Ether Lipid Biosynthesis in Archaea

Samta Jain,[1,2,4] Antonella Caforio,[1,2] Peter Fodran,[3] Juke S. Lolkema,[1,2] Adriaan J. Minnaard,[3] and Arnold J.M. Driessen[1,2,*]

[1]Department of Molecular Microbiology, Groningen Biomolecular Sciences and Biotechnology Institute, University of Groningen, 9747 AG Groningen, the Netherlands

[2]Zernike Institute for Advanced Materials, University of Groningen, 9747 AG Groningen, the Netherlands

[3]Stratingh Institute for Chemistry, University of Groningen, Nijenborgh 7, 9747 AG Groningen, the Netherlands

[4]Present address: Department of Medicine, Section of Infectious Diseases, Boston University School of Medicine, Boston, MA 02118, USA

*Correspondence: a.j.m.driessen@rug.nl

http://dx.doi.org/10.1016/j.chembiol.2014.07.022

SUMMARY

Archaeal membrane lipid composition is distinct from Bacteria and Eukarya, consisting of isoprenoid chains etherified to the glycerol carbons. Biosynthesis of these lipids is poorly understood. Here we identify and characterize the archaeal membrane protein CDP-archaeol synthase (CarS) that catalyzes the transfer of the nucleotide to its specific archaeal lipid substrate, leading to the formation of a CDP-activated precursor (CDP-archaeol) to which polar head groups are attached. The discovery of CarS enabled reconstitution of the entire archaeal lipid biosynthesis pathway in vitro, starting from simple isoprenoid building blocks and using a set of five purified enzymes. The cell free synthetic strategy for archaeal lipids we describe opens opportunity for studies of archaeal lipid biochemistry. Additionally, insights into archaeal lipid biosynthesis reported here allow addressing the evolutionary hypothesis of the lipid divide between Archaea and Bacteria.

INTRODUCTION

Glycerol linked hydrocarbon chains constitute the cellular membrane lipid composition of all living organisms. However, the versatility of this composition fundamentally distinguishes Archaea from Bacteria and Eukarya. The bacterial and eukaryotic membrane lipids are mostly composed of an *sn*-glycerol-3-phosphate (*sn*G-3-P) backbone esterified to linear fatty acids. On the other hand, the archaeal membrane lipids are characterized by an *sn*-glycerol-1-phosphate (*sn*G-1-P) backbone etherified to linear isoprenoids. This membrane lipid divide is considered evolutionarily very significant, and implicated in the differentiation of archaea and bacteria. It is not known why and how this differentiation occurred, and whether the two phospholipid biosynthesis pathways originated independently or from an ancestral cell with a heterochiral membrane lipid composition (Lombard et al., 2012a). Understanding the biosynthetic pathways leading to the formation and regulation of membrane lipid composition would help decipher the unknown aspects of early evolution. Although ether phospholipids or fatty acid based ether lipids are also found in a few bacteria and eukarya (Lorenzen et al., 2014), they differ from the isoprenoid derived archaeal ether lipids. The unique structure of archaeal membrane lipids is believed to be vital for the adaptation of these organisms to the extreme environmental conditions (Koga and Morii, 2007; van de Vossenberg et al., 1998), but this basic lipid architecture is found in all archaea including the mesophilic Thaumarchaeota. Among archaea, a great diversity of lipids exists derived from the basic diether structure *sn*-2,3-diphytanylglycerol diether called archaeol. A frequent modification of archaeol is the formation of the dimeric tetraether structure called caldarchaeol, which is prevalent in hyperthermophilic archaea and mesophilic Thaumarchaeota (Matsumi et al., 2011). Due to its unique membrane lipid composition, studies on the lipid biosynthetic pathway of archaea (Figure 1) are of particular interest. Crucial steps of the pathway from isoprenoid biosynthesis leading to the formation of unsaturated archaetidic acid have been investigated in detail. However, certain key enzymes (Lombard et al., 2012b; Villanueva et al., 2014) have not yet been identified, precluding a complete reconstitution of the pathway, while in vitro studies are hampered by the difficulty to acquire specific substrates.

In archaea, the biosynthesis of the isoprenoid building blocks isopentenyl pyrophosphate (IPP) and dimethylallyl pyrophosphate (DMAPP) occurs via the mevalonate pathway (Matsumi et al., 2011). The sequential condensation of IPP and DMAPP leads to the formation of an appropriate isoprenoid chain length of either geranylgeranyl (C20) and/or farnesylgeranyl (C25) diphosphate, involving enzymatic steps catalyzed by geranylgeranyl diphosphate (GGPP) synthase and farnesylgeranyl diphosphate synthase, respectively (Tachibana et al., 1993, 2000). These enzymes belong to a wide-spread family of *E*-isoprenyl diphosphate synthases (Wang and Ohnuma, 1999) that is also found in bacteria and plays a role in the biosynthesis of quinones and pigments (Nowicka and Kruk, 2010; Wang and Ohnuma, 1999). The *sn*G-1-P backbone is synthesized by the enzyme glycerol-1-phosphate dehydrogenase (G1PDH) that

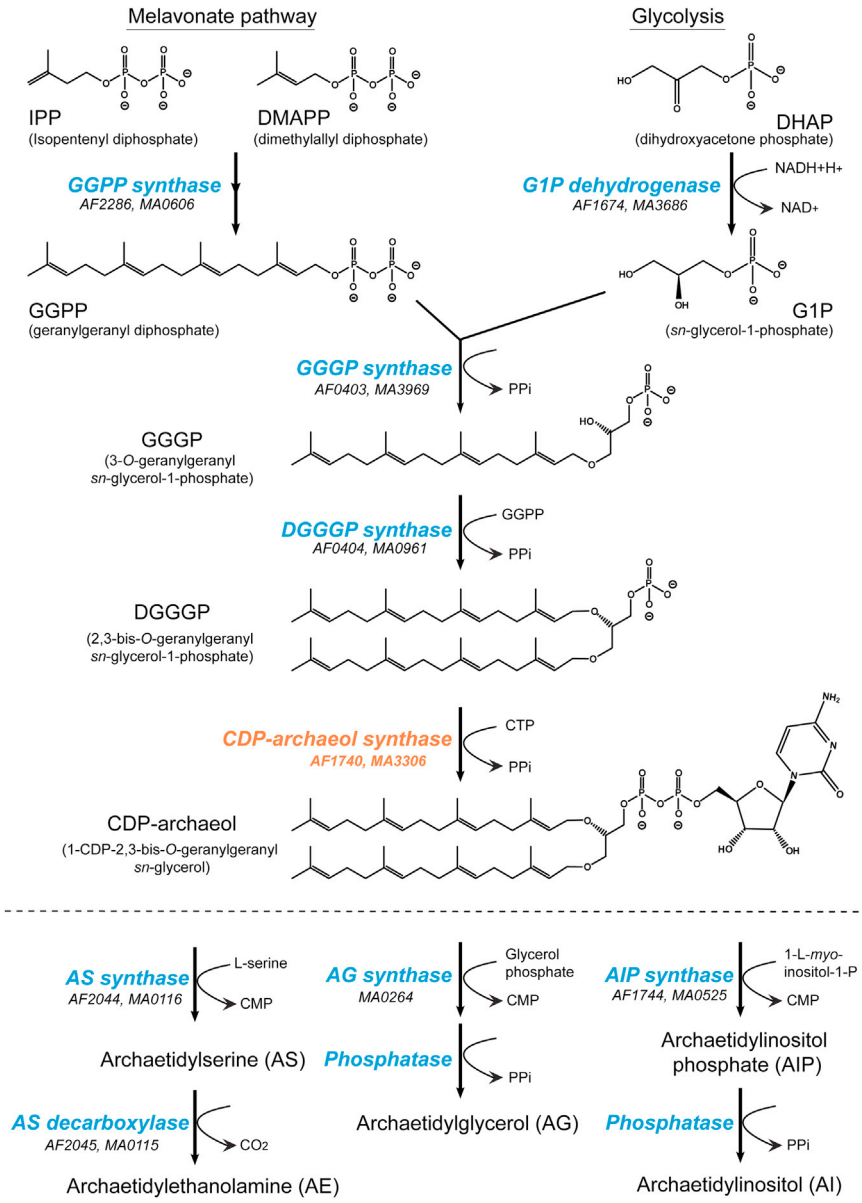

Figure 1. Archaeal Lipid Biosynthetic Pathway

Enzymes of the pathway are colored blue. CDP-archaeol synthase colored in orange is as identified in this study. Below the dashed line is the proposed pathway for polar head group attachment. The genes from Euryarchaea *A. fulgidus* and *Methanosarcina acetivorans* are indicated. The enzyme for the hydrogenation of the double bonds (AF0464 and MA1484) is not included since it is unclear at which step in the pathway the hydrogenation occur.

converts dihydroxyacetone phosphate (DHAP) to *sn*G-1-P using nicotinamide adenine dinucleotide (NADH) or the reduced form of Nicotinamide adenine dinucleotide phosphate as coenzyme (Han et al., 2002; Nishihara and Koga, 1997). The archaeal G1PDH enzymes share sequence similarity with alcohol and glycerol dehydrogenases, but belong to a different enzyme family than bacterial glycerol-3-phosphate dehydrogenases (Koga and Morii, 2007).

The two ethers that link the isoprenoid chains to carbon 3 and 2 of the *sn*G-1-P backbone are formed by two enzymes of the prenyl transferase family. The first enzyme is a cytoplasmic geranylgeranylglyceryl phosphate synthase (GGGP synthase), and the second enzyme is the membrane bound digeranylgeranylglyceryl phosphate synthase (DGGGP synthase). GGGP synthases are conserved in archaea, but also occur in some bacteria, they are phylogenetically divided into two groups (Nemoto et al., 2003; Peterhoff et al., 2014). They fulfill an evolutionarily central reaction by mediating the three characteristic features of the ether lipid structure, selectively joining the *sn*G-1-P enantiomer, rather than *sn*G-3-P, to the isoprenoid chain via an ether linkage. The crystal structure of the group I GGGP synthase from *Archaeoglobus fulgidus* shows a dimeric structure with a triose phosphate isomerase-barrel fold (Payandeh et al., 2006) bound to *sn*G-1-P, while the archaeal group II GGGP synthases show a similar structure, but they form higher order oligomers with modified G1P binding pocket (Peterhoff et al., 2014; Soderberg et al., 2001). The reaction forming the product 3-*O*-geranylgeranylglyceryl phosphate (GGGP) leads to the release of pyrophosphate and is Mg^{2+} dependent (Liang et al., 1992; Payandeh et al., 2006). The second ether bond is formed by the membrane protein DGGGP synthase that belongs to the UbiA prenyltransferase family. DGGGP synthase of *Sulfolobus solfataricus* was expressed in *E. coli*, and the enzymatic activity of the purified protein was found to be specific for the substrates GGPP and GGGP (Hemmi et al., 2004) synthesizing the product 2,3-di-*O*-geranylgeranylglyceryl phosphate (DGGGP). In a later study, DGGGP synthase was shown to accept both the S and R form of GGGP, thus being rather enantio unselective (Zhang et al., 2006).

For polar head group attachment, a CDP activated precursor is required. In Bacteria and Eukarya, the analogous reaction is catalyzed by the enzyme CDP-diacylglycerol synthase that binds the substrates CTP and phosphatidic acid and releases the products PP_i and CDP-diacylglycerol (Kelley and Carman, 1987; Sparrow et al., 1985). CDP-diacylglycerol is the central intermediate in the biosynthesis and regulation of phospholipids in Bacteria (Dowhan, 1997, 2013) and in Eukarya (Carman and Han, 2011; Chang and Carman, 2008; Heacock and Agranoff, 1997), in particular for the biosynthesis of phosphatidylinositol; phosphatidylglycerol; and in some organisms phosphatidylserine (Martin et al., 2000). It is believed that in Archaea a similar

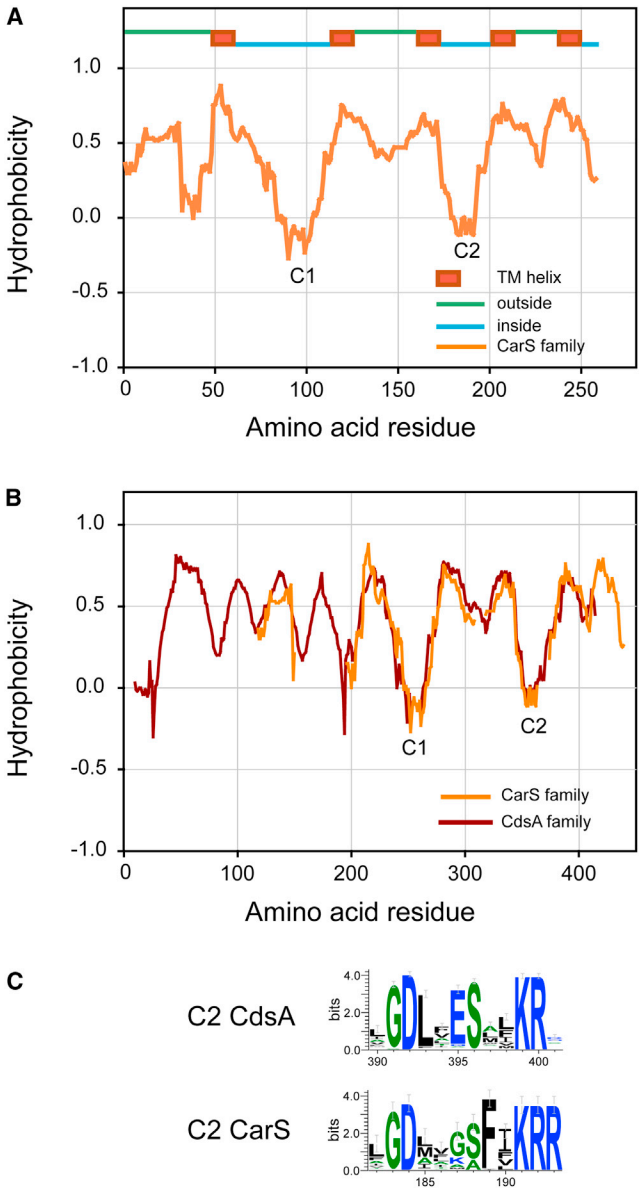

Figure 2. Hydrophobicity Profile of the Family of CarS and CdsA Proteins

(A) The averaged hydropathy profile (orange line) of the CarS family (Table S1) based on a multiple sequence alignment of 45 members those share between 20% and 60% sequence identity (see Figure S1 for multiple sequence alignment). The membrane topology model is depicted above the plot. Cytoplasmic loops (C1 and C2) are indicated. The structure divergence score (SDS) (Lolkema and Slotboom, 1998b), which is a measure of the similarity of the individual profiles, was 0.139. For phylogenetic tree distribution, see Figure S2.

(B) Hydropathy profile alignment of the CdsA (maroon) and CarS (orange) families. The averaged hydropathy profile (maroon line) of the CdsA family was based on 234 sequences sharing identity between 20% and 69%. The profile alignment reveals a similar pattern at the C terminus half with an *S* score of 0.83 (Lolkema and Slotboom, 1998b) (Figure S1 shows sequence alignment of CarS with six bacterial homologs).

(C) Conserved sequence motif of the C2 region of CdsA and CarS family is generated using WebLogo (Crooks et al., 2004), where the overall height represents the sequence conservation, and the height of each amino acid indicates its relative frequency of occurrence at that position.

reaction takes place in which CDP is transferred to the unsaturated archaetidic acid DGGGP, forming CDP-archaeol. Biochemical studies using membrane fractions of the archaeon *Methanothermobacter thermoautotrophicus* indicated an activity wherein [^{3}H]-CTP was incorporated into a lipid extractable fraction in the presence of DGGGP. The reaction was found to be Mg^{2+} dependent and was specific for the archaetidic acid substrates. Trace amounts of the compound CDP-archaeol were detected in cells of *M. thermoautotrophicus* (Morii et al., 2000). Although this suggests the occurrence of CDP-archaeol synthase activity in this organism, the gene encoding the enzyme in *M. thermoautotrophicus* or other archaea has remained elusive.

Here we report the identification and characterization of the key enzyme CDP-archaeol synthase of the ether lipid biosynthesis pathway that is ubiquitously present in Archaea. In conjunction with the other enzymes of this pathway, the synthesis of CDP-archaeol could be reconstituted in vitro using purified enzymes and simple building blocks.

RESULTS

Bioinformatics Analysis of Putative CDP-Archaeol Synthase

Except for the predicted CDP-archaeol synthase, all enzymes involved in the formation of archaeol have been identified, including enzymes for the hydrogenation of the double bonds (Isobe et al., 2014) and the polar head group attachment (Figure 1). A National Center for Biotechnology Information-BLAST analysis was carried out using the bacterial CDP-diacylglycerol synthase (CdsA) as query against the archaeal kingdom to identify candidate proteins with possible CDP-archaeol synthase activity. Further analysis of the retrieved sequences resulted in an extended list of conserved hypothetical proteins. These proteins belong to a family of unknown function (DUF46), contain several predicted transmembrane segments, and are found in all archaea except the phylum Nanoarchaeota and in three families of the phylum Thaumarchaeota. The domain of unknown function (DUF) region of the putative CDP-archaeol synthases spans more than two thirds of the entire protein sequence. Multiple sequence alignment indicates conserved residues mostly in the predicted cytoplasmic loop regions (C1 and C2) and the extreme C terminus, while the sequence conservation at the amino terminus is low (Figure S1 available online). The DUF46 family is grouped in the same clade (CTP-transferase like superfamily of the Pfam database) as the CTP-transferase 1 family that encompasses the bacterial CdsA protein. This indicates sequence or structure conservation among the two families as also recognized in a recent bioinformatics study (Lombard et al., 2012b).

To this end, a secondary structure analysis was performed by aligning the family averaged hydropathy profile of the CdsA and DUF46 families. Hydropathy profiles are evolutionarily better conserved than the primary amino acid sequence, providing a measure of the structural similarity of a membrane protein family (Lolkema and Slotboom, 1998a). The alignment of the archaeal family profile showed a common pattern with five predicted transmembrane domains (TMDs) and an extracellular amino-terminus (Figure 2A). The bacterial CdsA sequences are longer than

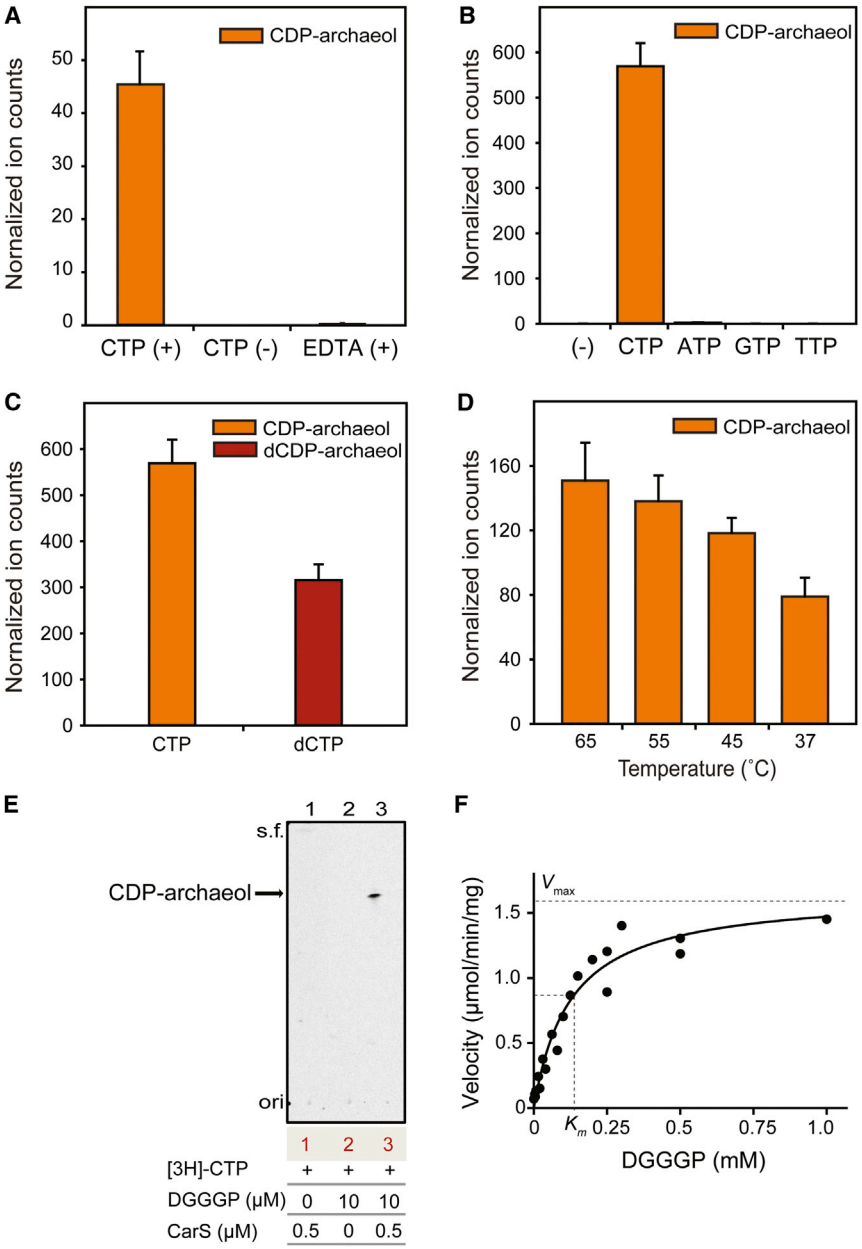

Figure 3. Characterization of CarS Activity

(A) In vitro reactions performed using purified CarS (Figure S3) and chemically synthesized substrate DGGGP (10 μM), product CDP-archaeol formation (m/z = 1,020.55 $[M-H]^-$) was analyzed by LC-MS.

(B) Nucleotide specificity of CarS examined for CTP, ATP, TTP, and GTP in the reaction.

(C) CarS activity measured using CTP or dCTP in a reaction to detect the formation of CDP-archaeol and dCDP-archaeol (m/z = 1,004.55 $[M-H]^-$).

(D) Enzymatic activity of CarS measured at different temperatures; the reaction was performed for 5 min.

(E) TLC autoradiogram of chloroform extractable lipid fraction from in vitro reactions, single spot of $[^3H]$-CDP-archaeol observed in lane 3; solvent front (s.f.) and origin (ori).

(F) Kinetic analysis of CarS using different substrate concentrations at 65°C for 5 min, the conversion of $[^3H]$-CTP to lipid (see Figure S3 for Lineweaver-Burk plot). Unless specified, the reactions were performed for 1 hr at 37°C with 0.5 μM CarS, 100 μM DGGGP, and 2 mM nucleotides. Total ion counts from LC-MS data were normalized using DDM as internal standard. LC-MS data are the average of three experiments ± SE.

the archaeal ones, containing additional TMDs at the N-terminal end that are poorly conserved. However, six bacterial sequences were retrieved that are shorter and display homology to the archaeal sequences (Figure S1). Interestingly, the alignment of the archaeal with the bacterial hydrophobicity profile indicates overlapping transmembrane segments and cytoplasmic loop regions at the carboxy-terminal half of the proteins (Figure 2B), in spite of low sequence similarity. Analysis of cytoplasmic loop C2 revealed a consensus sequence (G/S)Dxxx(S/A)xxKR conserved between the two families (Figure 2C). The hypothetical proteins displayed no conserved gene context and only a single copy per genome was retrieved for each sequence. The phylogenetic tree distribution (Figure S2) and a detailed list of the hypothetical proteins from all the sequenced genomes of archaea can be found in Table S1. The bioinformatics analysis suggests that the hypothetical protein may function as a CDP-archaeol synthase, and it was designated as CarS.

Identification and Characterization of CDP-Archaeol Synthase

The amino acid sequence of CarS from *Archaeoglobus fulgidus* was codon optimized for the overexpression in *E. coli*. An octa-histidine tag was introduced at the C terminus of CarS and the protein was overexpressed in *E. coli* Lemo21-DE3 strain under the control of T7 promoter and purified by Ni-nitrilotriacetic acid (NTA) affinity chromatography after solubilization of the membranes with the detergent n-dodecyl-β-D-maltopyranoside (DDM). On an SDS-PAGE gel, CarS showed a slightly anomalous running behavior than its theoretical molecular weight as expected for a polytopic membrane protein (Figures S3 and 5A). The protein was additionally identified by peptide mass fingerprinting using liquid chromatography-tandem mass spectrometry (LC-MS/MS) to confirm the amino acid sequence (Figure S3) and western blotting using α-his antibody (Figure S3). To examine the activity of the purified CarS protein, we chemically synthesized the substrate DGGGP and confirmed its structure using nuclear magnetic resonance (NMR) as described in Supplemental Experimental Procedures. In an in vitro reaction using purified CarS, the formation of the product CDP-archaeol from the substrate DGGGP was observed in the presence of CTP and Mg^{2+} by LC-MS (mass/charge [m/z]=1,020.55 $[M-H]^-$), while the product was absent in the EDTA (+) control reaction (Figures 3A and S3). The nucleotide

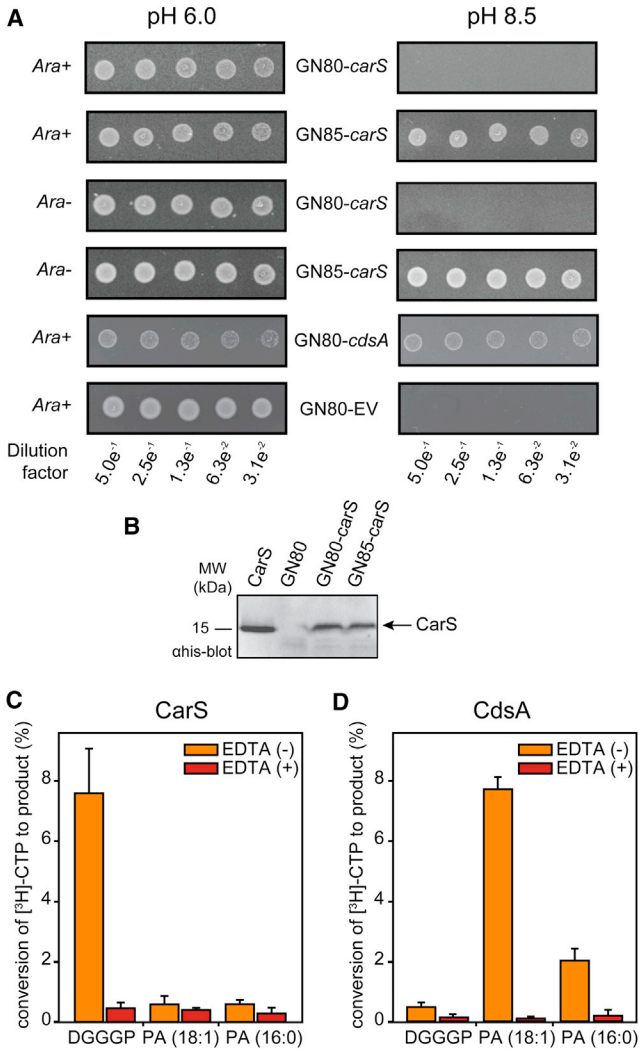

Figure 4. *carS* Cannot Complement *cdsA* Lethal Mutant Phenotype

(A) Serial dilutions (OD_{600} 0.3) of *E. coli* pH sensitive GN80 (*cdsA*$^-$) strain and its isogenic wild-type strain GN85 (*cdsA*$^+$) expressing *A. fulgidus carS, E. coli cdsA*, or EV were spotted on LB plates at pH 6.0 and pH 8.5. Arabinose (0.1%) was used to induce the expression.

(B) The total membrane fraction of the specified strains were analyzed for the expression of CarS (C terminus his tag) by immunoblotting with α-his antibody, purified CarS was used as a control.

(C and D) In vitro reactions with purified CarS (C) or CdsA (D) and various lipid substrates were performed using radiolabeled [^{3}H]-CTP. EDTA (+) reactions were used as controls. Liquid scintillation counts from the chloroform extractable fraction were used as a measure of the product formation. Data are the average of three experiments ± SE.

specificity of CarS for CTP was analyzed and no product formation was observed when ATP, guanosine-5'-triphosphate (GTP), or thymidine triphosphate (TTP) was used instead of CTP (Figure 3B). When the reaction was incubated in the presence of deoxycytidine triphosphate (dCTP), the spectral analysis revealed the presence of a product identified as deoxycytidine diphosphate (dCDP)-archaeol (m/z=1,004.55 [M-H]$^-$), at almost the same retention time as CDP-archaeol (Figures 3C and S3). This result indicates that the absence of a hydroxyl group on the 2′ position of the ribose moiety of CTP does not affect the enzymatic activity as reported earlier for the *E. coli* CdsA (Sparrow et al., 1985). CarS used in this study was derived from a thermophile. Consequently, the rate of product formation was found to be higher at 65°C when compared to lower temperatures (37°, 45°, and 55°C) (Figure 3D).

The activity of CarS was also determined using [^{3}H]-CTP, where the chloroform extractable lipid fraction from the reaction was analyzed by thin layer chromatography (Morii et al., 2000). A single spot of radiolabeled CDP-archaeol was observed only in the presence of DGGGP (Figure 3E). Next, the CarS activity was measured at different concentrations of substrate DGGGP using [^{3}H]-CTP. Normal saturation kinetic was obtained when the data were fitted to Michaelis-Menten equation using nonlinear regression and an apparent K_m=0.12 ± 0.02 mM and k_{cat}=0.55 ± 0.03 s^{-1} was observed (Figure 3F). Furthermore, no significant deviation from linearity was observed when the data were fitted using Lineweaver-Burk plot (Figure S3). Taken together, these data demonstrate that CarS functions as a CDP-archaeol synthase.

CarS Has a Distinct Activity versus CdsA

CDP-diacylglycerol synthase (CDS) is a ubiquitous and essential enzyme as shown previously in bacterial and eukaryal systems (Dowhan, 1997; Heacock and Agranoff, 1997; Shen et al., 1996). A conditionally lethal strain of *E. coli* with a mutant *cdsA* gene (GN80) cannot grow at pH values above 8.0, showing greatly reduced CdsA activity and the accumulation of the substrate phosphatidic acid (PA) at levels around 30% of the total lipid composition compared to 0.2% in the wild-type (Ganong and Raetz, 1982). Previous studies have shown that the *Drosophila CDS* gene expression could rescue the *E. coli cdsA* mutant pH sensitive phenotype (Dowhan, 1997; Wu et al., 1995), although the eukaryotic CDS has a longer amino acid sequence than the bacterial homolog. To examine this possibility also for the archaeal CarS, a complementation study was performed. *A. fulgidus carS* could not restore the growth defect of *E. coli* GN80 (*cds*$^-$) strain at pH 8.5, while the *E. coli cdsA* could complement the growth defect of the *E. coli* GN80 (*cds*$^-$) strain (Figure 4A). As a control, the isogenic wild-type *E. coli* GN85 (*cds*$^+$) strain was also used and the expression level of CarS was found unaltered between the two strains (Figure 4B).

To measure the specificity of *A. fulgidus* CarS and *E. coli* CdsA for their respective lipid substrates DGGGP and PA in vitro, *E. coli* CdsA was overexpressed and purified (Figure S3), and the assay was performed using radiolabeled [^{3}H]-CTP. Since the enzymatic activity of CarS and CdsA is Mg^{2+} dependent, EDTA (+) was used as a control for each reaction and the chloroform extractable lipid fraction of the reaction was measured. When CarS was incubated either with PA 18:1 (oleic acid) or PA 16:0 (palmitic acid) (Figure 4C), only a very low background signal (<1%; likely spill over of radioactivity originating from incomplete phase separation) was detected in EDTA (+) control that did not differ from the reaction without EDTA. A very low activity was observed when CdsA was incubated with DGGGP in the reaction, whereas high levels of activity occurred with PA (18:1 and 16:0) (Figure 4D). These data demonstrate that CarS and CdsA have distinct substrate specificities.

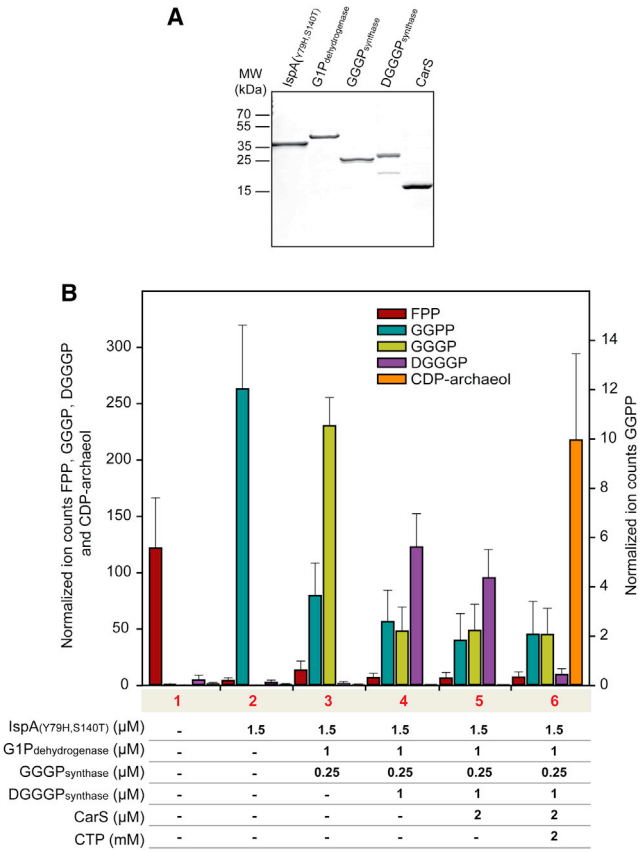

Figure 5. In Vitro Conversion of Isopentenyl Pyrophosphate and Farnesyl Diphosphate to CDP-Archaeol

(A) Coomassie stained SDS-PAGE gels showing the Ni-NTA purified proteins from different sources overexpressed in *E. coli*. IspA(Y79H and S140T) mutant of *E. coli* (33 kDa), G1P dehydrogenase of *B. subtilis* (44 kDa), GGGP synthase of *M. maripaludis* (29 kDa), DGGGP synthase of *A. fulgidus* (34 kDa), and CarS of *A. fulgidus* (20 kDa). For the description and activities of the individual proteins, see Table S2 and Figure S4.

(B) In vitro reactions were performed using purified proteins as specified and the substrates IPP, FPP, DHAP, and NADH in the presence of Mg^{2+} and 0.1% DDM. The products were extracted and analyzed by LC-MS. The spectral data constituting total ion counts (measured as peak area using Thermo Scientific XCalibur processing software) of the products FPP (m/z = 381), GGPP (m/z = 449.19 $[M-H]^-$), GGGP (m/z = 443.26 $[M-H]^-$), DGGGP (m/z = 715.51 $[M-H]^-$), and CDP-archaeol (m/z = 1,020.55 $[M-H]^-$) were normalized using DDM (m/z = 509.3 $[M-H]^-$) as internal standard and plotted on the y axis. Data of GGPP is plotted on the secondary y axis. The graph represents average of three experiments ± SE, see Figure S4 for the total ion counts and Figure S5 for the TLC based quantitation of the metabolites.

Enzymatic Conversion of the Precursors Isopentenyl Pyrophosphate and Farnesyl Diphosphate to CDP-Archaeol

To reconstitute the complete ether lipid biosynthesis pathway in vitro, enzymatic reactions were performed using a combination of five purified proteins of which three are encoded by archaea and two by bacteria as described in Table S2. The archaeal enzymes GGGP synthase, DGGGP synthase, and CarS were codon optimized for the overexpression in the host *E. coli*. For the expression of DGGGP synthase, a synthetic ribosome-binding site was introduced that greatly enhanced the expression levels (Salis et al., 2009). The various enzymes were purified from the DDM-solubilized membrane fraction (DGGGP synthase and CarS) or the cytosolic fraction (IspA(Y79H, S140T), G1P dehydrogenase, and GGGP synthase) by Ni-NTA affinity column (Figure 5A). Isoprenoid building blocks IPP and DMAPP undergo serial condensation to form oligomers of defined chain lengths (C10, C15, C20, etc.) (Wang and Ohnuma, 1999). In archaea, GGPP synthase catalyzes the formation of (C20 and GGPP). Mutants of its *E. coli* homolog IspA (farnesyl diphosphate [FPP] synthase) were shown previously to synthesize GGPP instead of farnesyl diphosphate (C15 and FPP) (Lee et al., 2005). There was one such mutant IspA(Y79H and S140T) that was generated in this study and shown to catalyze the conversion of IPP and FPP to GGPP (m/z=449.19 $[M-H]^-$) as measured by LC-MS (Figure 5B, lane 2).

Recently, it was discovered that the enzyme G1P dehydrogenase, responsible for the stereo-specificity of archaeal lipids, is also encoded by certain bacteria (Guldan et al., 2011). Of these, AraM of *Bacillus subtilis* was functionally characterized and shown to perform the same reaction as the archaeal homolog, thereby synthesizing G1P from DHAP and NADH (Guldan et al., 2008). In our study, we thus expressed G1P dehydrogenase (AraM) of *B. subtilis* in *E. coli* and purified the enzyme accordingly (Figure 5A, lane 2). The G1P dehydrogenase was catalytically active in an NADH oxidation assay using DHAP and NADH as substrates as described previously (Guldan et al., 2008) (Figure S4).

GGGP synthase catalyzes the first ether formation between the substrates GGPP and G1P, leading to the synthesis of the compound GGGP (Payandeh et al., 2006). Like the other enzymes of the family (Soderberg et al., 2001), GGGP synthase of *M. maripaludis* also purifies as a higher order oligomer (data not shown). Its activity was established using an in vitro reaction where formation of the product GGGP (m/z=443.26 $[M-H]^-$) was detected in LC-MS only after addition of the substrates GGPP and racemic G1P (rG1P) (Figure S4). When GGGP synthase was added to the reaction in combination with enzymes IspA(Y79H and S140T) and G1P dehydrogenase and in the presence of substrates IPP, FPP, DHAP, and NADH, formation of the product GGGP and consumption of GGPP was observed (Figure 5B, lane 3).

The second ether is formed by the first integral membrane protein of the pathway, DGGGP synthase, using substrates GGGP and GGPP (Hemmi et al., 2004). In this study, DGGGP synthase encoded by *A. fulgidus* was first monitored in a reaction added in different ratios to the *M. maripaludis* GGGP synthase, the common substrate GGPP and rG1P for the formation of the product DGGGP (m/z=715.51 $[M-H]^-$) (Figure S4). In a subsequent coupled reaction with the other enzymes of the pathway, DGGGP synthase dependent formation of DGGGP was observed (Figure 5B, lane 4). The subsequent reactions were performed in the presence of CarS where a CTP dependent synthesis of CDP-archaeol was only detected in conjunction with other enzymes (Figure 5B, lanes 5 and 6). No other unique products were found while comparing the LC-MS spectral data of reactions in lanes 5 and 6 indicating that CarS does not utilize GGGP as a substrate. The total ion counts acquired for each product during the LC-MS analysis of the assay are shown in Figure S4.

To estimate the amount of different metabolites formed in these reactions, a similar assay was performed using radiolabeled substrate [^{14}C]-IPP, and the products were analyzed by thin-layer chromatography (TLC) (Figure S5). Quantitation of the spots revealed that picomole amounts of products were formed in a 100 μl reaction starting with 90 pmoles of [^{14}C]-IPP indicating an efficient conversion (Figure S5). The data showed a similar spectrum of metabolites being formed in the different reactions as observed for the LC-MS based analysis. TLC analysis further confirmed that CarS does not utilize GGGP as substrate.

The reaction described here thus constitutes the biosynthetic route of the archaeal lipid precursor CDP-archaeol formation (Figure 1), establishing the role of CarS in context with the other enzymes of the pathway.

DISCUSSION

CDP-activated precursors are important intermediates in the biosynthesis of phospholipids in bacteria and eukarya and are subsequently modified in various pathways for polar head group attachment. It is synthesized by the conserved and essential enzyme CDP-diacylglycerol synthase (Ganong and Raetz, 1982). In this study, we elucidated the formation of the CDP-activated precursor CDP-archaeol, the uncharacterized key step in the lipid biosynthetic pathway of archaea. The enzyme required for its synthesis in archaea, CarS, was identified and characterized in vitro. Bioinformatics analysis of CarS homologs indicated a conserved hypothetical protein in the kingdom archaea with remote homology to the bacterial CdsA as predicted previously (Lombard et al., 2012b). Structure analysis by the hydropathy profile alignment revealed a partial fold similarity between the two families that share conserved aspartate, lysine, and arginine residues in the cytoplasmic loop (C2) region where they may be involved with the CTP associated activity of the enzyme. Bacterial CdsA proteins are longer than the archaeal CarS, with their N-terminal region less conserved and of unknown function. Interestingly, the homologous eukaryotic CDS proteins are even longer, having an extended N-terminal hydrophilic region. However, six bacterial sequences with shorter length and high sequence similarity to archaeal CarS were retrieved suggesting an event of horizontal gene transfer.

The CarS sequence was retrieved from all sequenced genomes of archaea, with some exceptions. It is not present in the phyla Nanoarchaeota, which is a symbiont that encodes no genes of the lipid biosynthetic pathway (Podar et al., 2013). The lack of CarS sequence in the three families of the phylum Thaumarchaeota (where CarS is found only in the unclassified family *Candidatus Caldiarchaeum subterraneum*) is intriguing since they contain ether lipids. In our analysis, we retrieved GGGP synthase sequences from these families, but not the DGGGP synthase sequences which is recently reported to exhibit high sequence divergence in Thaumarchaeota where it might be related to the synthesis of cyclohexane moiety specific to Thaumarchaeota lipid structure (Villanueva et al., 2014). We therefore hypothesize that the CarS is also poorly conserved in these organisms and thus difficult to identify. Another possibility could be that an additional enzyme with low sequence homology performs the same function, a situation similar to what was observed previously for folate biosynthesis in archaea (de Crécy-Lagard et al., 2012).

In this study, we used the chemically synthesized unsaturated archaetidic acid DGGGP as substrate to examine the enzymology of CarS. Biochemical investigation performed with purified CarS and DGGGP clearly showed CTP dependent formation of the product CDP-archaeol. Similar to CdsA, CarS uses metal (Mg^{2+}) ions for coordination, accepts CTP and dCTP as substrate, and does not utilize ATP, GTP, or TTP nucleotides in the reaction. The apparent K_m for DGGGP (measured with constant detergent concentration) was calculated as 0.12 ± 0.02 mM, which only serves as an indication for the affinity toward the lipid substrate due to the presence of detergent in the reaction. The K_m for PA of CDS from various organisms has been studied before and in general ranges from 0.28 mM (*E. coli*) to 0.9 mM (*Plasmodium falciparum*) (Martin et al., 2000; Shastri et al., 2010), and thus the K_m of CarS for DGGGP compares favorable with those studies. In some studies, the K_m was measured in constant lipid:detergent ratio, thereby taking surface dilution kinetics (Carman et al., 1995) into account. However, in those cases, the influence of detergent variation on the activity of the protein cannot be excluded. *A. fulgidus carS* could not complement the pH sensitive *E. coli cdsA*$^-$ phenotype in vivo, while the enzyme CarS also did not accept PA as a substrate in the in vitro reactions, thereby distinguishing the archaeal and bacterial enzymes for their lipid substrate specificity.

Having identified the fate of DGGGP in the pathway, we attempted to reconstitute the conversion of IPP to CDP-archaeol in vitro. This technically challenging aspect of the study was accomplished by selecting the appropriate combination of enzymes for the reaction. Several proteins were individually screened for expression, purification, and activity. The *E. coli* IspA and archaeal GGPP synthase belong to the prenyl transferase family that have two highly conserved aspartate rich regions called the FARM and SARM domains. Mutations close to these domains lead to alteration in product length formation probably due to change in the hydrophobic pocket of the enzyme (Wang and Ohnuma, 1999). IspA(Y79H and S140T) mutant described previously (Lee et al., 2005) was therefore selected with the Y79 residue being five amino acids upstream of the FARM domain. The *B. subtilis* AraM is the only characterized bacterial G1P dehydrogenase, but homologs are found in several other bacteria as hypothetical proteins (Guldan et al., 2008). G1P in *B. subtilis* is further converted into an archaea type lipid (heptaprenylglyceryl phosphate), the physiological function of which is still unknown (Guldan et al., 2011; Peterhoff et al., 2014). The *E. coli* IspA mutant and *B. subtilis* AraM were used in our study for the optimum overexpression in the host *E. coli* compared to their instable archaeal homologs that readily form inclusion bodies (S.J., unpublished data). Here we report on the activity of the purified GGGP synthase encoded by *M. maripaludis*, a methanogen that grows at 37°C. Like the other archaeal species (Nemoto et al., 2003; Payandeh et al., 2006; Peterhoff et al., 2014; Soderberg et al., 2001), the GGGP synthase of *M. maripaludis* converts G1P and GGPP to GGGP and is purified as an oligomer. The archaeal membrane proteins DGGGP synthase and CarS encoded from *A. fulgidus*, a hyperthermophile, were selected for this study because they display higher expression levels and stability than the

methanogenic counterparts. The in vitro coupled reaction showing the conversion of archaeal lipid precursor IPP into CDP-archaeol demonstrates that all the enzymes are functional in detergent (DDM) and at 37°C. This holistic approach further establishes the enzymatic role of CarS in the archaeal lipid biosynthetic pathway.

The subsequent step of the pathway is polar head group attachment. Since the polar head groups are shared among the three domains of life, their biosynthesis is thought to be mediated in a similar manner (Koga and Morii, 2007; Lombard et al., 2012b). The enzymes for polar head group attachment that accept the CDP-activated precursors indeed belong to a large family called CDP-alcohol phosphatidyltransferase with homologs in bacteria and archaea, but their classification is unclear with mixed sequence distribution (Lombard et al., 2012b). Interestingly, the archaeatidyl serine synthase and the bacterial subclass II phosphatidylserine synthase were shown to even accept lipid substrates of each other, suggesting a broad substrate specificity and possibly common mechanism (Morii and Koga, 2003). In archaea, it is unclear at what step of the pathway the saturation of the membrane lipids takes place (Sasaki et al., 2011).

The strategy described here to synthesize archaeal lipids in a cell free manner paves the way for future studies on archaeal lipid biochemistry like the mechanism of tetraether linkage, sugar group attachment, cyclopentane and macrocyclic ring formation, and various other derivatives of the archaeal lipids. A further challenge is to reprogram bacterial ester-based lipid biosynthesis into ether-based lipids to test the evolutionary hypothesis of the lipid divide between Archaea and Bacteria (Lombard et al., 2012a).

SIGNIFICANCE

This study describes the identification and functional characterization of CarS, the enzyme of the archaeal ether lipid biosynthesis pathway. This enzyme is universally conserved among archaea and catalyzes the biosynthesis of the CDP-activated precursors (CDP-archaeol) needed for polar head group attachment. Further, a cell-free synthesis of archaeal phospholipids is performed by in vitro reconstitution of the entire lipid biosynthesis pathway of archaea using a set of five purified (membrane) enzymes, starting from simple isoprenoid building blocks into the CDP-archaeol. This study paves the way for future studies on enzyme mechanism, biosynthesis, and the molecular basis of the lipid-divide that distinguishes archaea from the other kingdoms of life.

EXPERIMENTAL PROCEDURES

Protein Expression and Purification

Proteins were overexpressed in *E. coli* BL21 strain and induced with 0.5 mM isopropyl β-D-1-thiogalactopyranoside (IPTG). For overexpression of CarS, the *E. coli* Lemo strain was used and induced using 0.4 mM of IPTG and 0.5 mM of L-rhamnose. After 2 hr of induction, the cells were harvested, washed with 50 mM Tris-HCl pH 7.5, and resuspended in the same buffer supplemented with 0.5 mg/ml of ribonucleases and deoxyribonucleases and complete EDTA free protease inhibitor tablet (Roche). The suspension was subjected to cell disruption at 13,000 psi and the cell lysate was centrifuged for 10 min at low speed (12,000×*g*) to remove unbroken cells. The cytoplasmic and membrane fractions were separated with high-speed centrifugation at (235,000×*g*) for 1 hr.

For the purification of soluble proteins (IspA(Y79H and S140T), G1P dehydrogenase, and GGGP synthase), the cytoplasmic fraction was incubated with Ni-NTA beads (Sigma) in buffer A (50 mM Tris-HCl pH 7.5, 150 mM NaCl, 10% glycerol) for 30 min at 4°C. The beads were washed five times with 20 column volumes (CV) of buffer A supplemented with 20 mM Imidazole and eluted two times with 2 CV of buffer A supplemented with 250 mM imidazole.

For purification of membrane proteins (DGGGP synthase, CarS, and CdsA), inner membrane vesicles (IMVs) of *E. coli* were isolated as described previously (Kaufmann et al., 1999) and resuspended in buffer A. The IMVs (1 mg/ml) were solubilized at 4°C for 1 hr in 2% of DDM detergent. Insolubilized materials were removed by centrifugation (173,400×*g*) for 30 min and the supernatant was incubated with Ni-NTA beads for 30 min at 4°C. The beads were washed five times with 40 CV of buffer B (0.2% DDM, 50 mM Tris pH 7.5, 150 mM NaCl, 10% glycerol), supplemented with 10 mM imidazole, and eluted three times with 0.5 CV of buffer B supplemented with 250 mM imidazole. The purity of the proteins was checked by 15% SDS-PAGE, stained with Coomassie brilliant blue. Absorbance was measured at 280 nm in a spectrophotometer to determine the concentration of purified protein.

In Vitro Assays for Lipid Synthesis

Reactions were performed using assay buffer with an end concentration of 50 mM Tris-HCl pH 7.5, 10 mM MgCl2, 75 mM NaCl, 0.1% DDM, 125 mM imidazole, and 5% glycerol. Where specified, 2 mM CTP, 20 mM EDTA, 0.25 mM NADH, 0.1 mM DHAP, 0.1 mM IPP, 0.1 mM FPP, 4 mM rG1P, and 0.1 mM GGPP were used in a 100 μl reaction volume. After incubation at specified temperature and time, the products were extracted two times with 0.3 ml *n*-butanol and evaporated under a stream of nitrogen gas. The samples were resuspended in 0.05 or 0.1 ml methanol and analyzed by LC-MS.

Assays Using Radionucleotides

Purified CarS or CdsA (0.5 μM) was incubated with specified amounts of DGGGP or 200 μM PA in assay buffer with 5 μCi [^{3}H]-CTP (1.68 μM) and 2 mM cold CTP in a 100 μl reaction volume. The reaction for lipid biosynthesis had same composition as described above for the LC-MS assay with the addition of 0.005 μCi [^{14}C]-IPP (0.9 μM) in a 100 μl reaction volume. The reaction was incubated for 5 min at 65°C (for kinetic measurements) or for 1 hr at 37°C. Acidic Bligh and Dyer extraction (Koga and Morii, 2006) was performed and the chloroform extractable lipid fraction was evaporated. The radioactivity was counted after the addition of 10 ml Emulsion Scintillation liquid (PerkinElmer) using Packard scintillation counter. When analyzed by thin layer chromatography, the samples were resuspended in 10 μl chloroform and spotted on Silica Gel 60 (Merck) plates. Solvents chloroform, methanol, 7 M ammonia in the ratio 60:35:8 (Morii et al., 2000) were used as mobile phase. Using phosphor screen or tritium sensitive phosphor screen, the autoradiograph was obtained by the phosphorimager (Roche). The spots were quantitated along with [^{14}C]-IPP dilution series using Image J software and the amounts were extrapolated using the [^{14}C]-IPP calibration curve.

Genetic Complementation

E. coli strains GN80 and GN85 (Ganong and Raetz, 1982) were transformed with two plasmids, pSJ122 (CarS under the control of T7 promoter) and pTara (Wycuff and Matthews, 2000) (under the control of *araBAD* promoter). In this manner, the addition of arabinose to the culture led to the controlled expression of T7 polymerase that subsequently led to the expression of CarS. For the controls, pSJ122 was replaced by pSJ148 (*E. coli* CdsA under the control of T7 promoter) or empty vector (EV) and transformed in GN80. To perform the pH sensitivity assay, serial dilutions of the transformants with optical density at 600 nm (OD_{600}) of 0.3 were plated on LB agar plates with pH 6.0 (pH adjusted using 50 mM 2-(N-morpholino)ethanesulfonic acid buffer) or pH 8.5 (pH adjusted using NaOH) that were prepared as described previously (Ganong and Raetz, 1982). Expression was induced by the addition of 0.1% arabinose.

Liquid Chromatography Mass Spectrometry

Samples were analyzed using an Accela1250 high-performance liquid chromatography system coupled with a bench top electrospray ionization mass

spectrometry (ESI-MS) Orbitrap Exactive (Thermo Fisher Scientific). A sample of 5 or 10 μl was injected into a COSMOSIL 5SL-II packed C4 column with dimensions 4.6 mm I.D. × 150 mm (Nacalai tesque) operating at 40°C with a flow rate of 500 μl/min. Eluents A (25 mM ammonium bicarbonate) and B (acetonitrile) were used as follows: −97% A isocratic for 5 min, gradient 97% A to 100% B (Acetonitrile) for 30 min, 100% B isocratic for 25 min, gradient 100% B to 97% A for 10 min, and 97% A isocratic for 5 min. The column effluent was injected directly into the Exactive ESI-MS Orbitrap operating in negative ion mode. Voltage parameters of 3 kV (spray), −52.5V (capillary), and −160 V (tube lens) was used. Capillary temperature of 300°C, sheath gas flow 60, and auxiliary gas flow of five was maintained during the analysis. For performing fragmentation, high-energy collision induced dissociation (HCD) gas was used at 35eV. Data analysis was performed using the Thermo XCalibur processing software for automated peak integration and quantification. The ICIS algorithm for component peak detection was applied in this analysis.

Chemical Synthesis of Unsaturated Archaetidic Acid, Gigeranylgeranylglyceryl Phosphate

DGGGP was chemically synthesized according to the scheme in Supplemental Experimental Procedures. Compound A was prepared as described previously (Dannenmuller et al., 2000). The (*S*)-1,2-isopropylidene glycerol was protected with a dimethoxybenzyl group, followed by hydrolysis of the acetonide and bis-alkylation with geranylgeranyl chloride. Oxidative deprotection with 2,3-dichloro-5,6-dicyanobenzoquinone afforded A. The phosphorylation of A proved to be surprisingly challenging, possibly due to the polyunsaturation of the geranylgeranyl side chains. Treatment of A with $POCl_3$ and subsequent hydrolysis led to decomposition. Phosphorylation using $(MeO)_2POCl$ as previously reported (Morii et al., 2000) gave the desired bismethoxy phosphoric ester B. However, the demethylation conditions described in that study using TMSBr led to decomposition of B. Other common P^V reagents could not be used because these require either hydrogenation or strongly acidic conditions for deprotection. An alternative viable approach toward the phosphorylated product G is phosphoramidite methodology (Caruthers et al., 1987). From a plethora of reagents reported for various purposes, we chose those that require relatively mild basic conditions for cleavage. Application of phosphoramidite C gave the desired bisprotected product D in 70% yield. The cyanoethyl groups were reported to undergo facile deprotection with an excess of a secondary or tertiary amine. However, this did not occur, although partial deprotection was observed. This led to application of the more base-sensitive phosphoramidite E bearing two 9-fluorenylmethyl groups (Watanabe et al., 1997). The desired bisprotected derivative F was obtained in an excellent 94% yield. The first 9-fluorenylmethyl group could be readily cleaved using an excess of Et_3N. After changing to more basic conditions, the remaining protecting group could be also removed. The desired phosphoric acid derivative F was obtained in 48% yield after column chromatography. Compared to the previously published synthesis with a yield of <6% (Morii et al., 2000), the procedure described here gave a higher yield (17%).

The detailed experimental protocol and NMR data are described in Supplemental Experimental Procedures.

SUPPLEMENTAL INFORMATION

Supplemental Information includes Supplemental Experimental Procedures, five figures, and three tables and can be found with article online at http://dx.doi.org/10.1016/j.chembiol.2014.07.022.

AUTHOR CONTRIBUTIONS

S.J. and A.D. conceived and designed the research; S.J. performed the in vivo complementation studies and in vitro reconstitution assays; A.C. purified and characterized CarS; J.L. performed the bioinformatics; A.M. designed the DGGGP synthesis, which was performed by P.F.; and the manuscript was written by the contributions of all authors.

ACKNOWLEDGMENTS

This project was carried out within the research program of the biobased ecologically balanced sustainable industrial chemistry (BE-BASIC). We are grateful to William Dowhan for providing us with the *E. coli* strains GN80 and GN85. We thank Oleksander Salo, Stephan Portheine, and Ilja Kusters for technical assistance. We extend our gratitude to John van der Oost, Melvin Siliakus, and Servè Kengen for fruitful discussions.

Received: June 11, 2014
Revised: July 22, 2014
Accepted: July 24, 2014
Published: September 11, 2014

REFERENCES

Carman, G.M., Deems, R.A., and Dennis, E.A. (1995). Lipid signaling enzymes and surface dilution kinetics. J. Biol. Chem. *270*, 18711–18714.

Carman, G.M., and Han, G.-S. (2011). Regulation of phospholipid synthesis in the yeast Saccharomyces cerevisiae. Annu. Rev. Biochem. *80*, 859–883.

Caruthers, M.H., Barone, A.D., Beaucage, S.L., Dodds, D.R., Fisher, E.F., McBride, L.J., Matteucci, M., Stabinsky, Z., and Tang, J.Y. (1987). Chemical synthesis of deoxyoligonucleotides by the phosphoramidite method. Methods Enzymol. *154*, 287–313.

Chang, Y.-F., and Carman, G.M. (2008). CTP synthetase and its role in phospholipid synthesis in the yeast Saccharomyces cerevisiae. Prog. Lipid Res. *47*, 333–339.

Crooks, G.E., Hon, G., Chandonia, J.-M., and Brenner, S.E. (2004). WebLogo: a sequence logo generator. Genome Res. *14*, 1188–1190.

Dannenmuller, O., Arakawa, K., Eguchi, T., Kakinuma, K., Blanc, S., Albrecht, A.M., Schmutz, M., Nakatani, Y., and Ourisson, G. (2000). Membrane properties of archaeal macrocyclic diether phospholipids. Chemistry *6*, 645–654.

de Crécy-Lagard, V., Phillips, G., Grochowski, L.L., El Yacoubi, B., Jenney, F., Adams, M.W.W., Murzin, A.G., and White, R.H. (2012). Comparative genomics guided discovery of two missing archaeal enzyme families involved in the biosynthesis of the pterin moiety of tetrahydromethanopterin and tetrahydrofolate. ACS Chem. Biol. *7*, 1807–1816.

Dowhan, W. (1997). CDP-diacylglycerol synthase of microorganisms. Biochim. Biophys. Acta *1348*, 157–165.

Dowhan, W. (2013). A retrospective: use of Escherichia coli as a vehicle to study phospholipid synthesis and function. Biochim. Biophys. Acta *1831*, 471–494.

Ganong, B.R., and Raetz, C.R. (1982). Massive accumulation of phosphatidic acid in conditionally lethal CDP-diglyceride synthetase mutants and cytidine auxotrophs of Escherichia coli. J. Biol. Chem. *257*, 389–394.

Guldan, H., Sterner, R., and Babinger, P. (2008). Identification and characterization of a bacterial glycerol-1-phosphate dehydrogenase: Ni(2+)-dependent AraM from Bacillus subtilis. Biochemistry *47*, 7376–7384.

Guldan, H., Matysik, F.-M., Bocola, M., Sterner, R., and Babinger, P. (2011). Functional assignment of an enzyme that catalyzes the synthesis of an archaea-type ether lipid in bacteria. Angew. Chem. Int. Ed. Engl. *50*, 8188–8191.

Han, J.-S., Kosugi, Y., Ishida, H., and Ishikawa, K. (2002). Kinetic study of sn-glycerol-1-phosphate dehydrogenase from the aerobic hyperthermophilic archaeon, Aeropyrum pernix K1. Eur. J. Biochem. *269*, 969–976.

Heacock, A.M., and Agranoff, B.W. (1997). CDP-diacylglycerol synthase from mammalian tissues. Biochim. Biophys. Acta *1348*, 166–172.

Hemmi, H., Shibuya, K., Takahashi, Y., Nakayama, T., and Nishino, T. (2004). (S)-2,3-Di-O-geranylgeranylglyceryl phosphate synthase from the thermoacidophilic archaeon Sulfolobus solfataricus. Molecular cloning and characterization of a membrane-intrinsic prenyltransferase involved in the biosynthesis of archaeal ether-linked membrane lipids. J. Biol. Chem. *279*, 50197–50203.

Isobe, K., Ogawa, T., Hirose, K., Yokoi, T., Yoshimura, T., and Hemmi, H. (2014). Geranylgeranyl reductase and ferredoxin from Methanosarcina acetivorans are required for the synthesis of fully reduced archaeal membrane lipid in Escherichia coli cells. J. Bacteriol. *196*, 417–423.

Kaufmann, A., Manting, E.H., Veenendaal, A.K., Driessen, A.J., and van der Does, C. (1999). Cysteine-directed cross-linking demonstrates that helix 3 of

SecE is close to helix 2 of SecY and helix 3 of a neighboring SecE. Biochemistry *38*, 9115–9125.

Kelley, M.J., and Carman, G.M. (1987). Purification and characterization of CDP-diacylglycerol synthase from Saccharomyces cerevisiae. J. Biol. Chem. *262*, 14563–14570.

Koga, Y., and Morii, H. (2006). Special methods for the analysis of ether lipid structure and metabolism in archaea. Anal. Biochem. *348*, 1–14.

Koga, Y., and Morii, H. (2007). Biosynthesis of ether-type polar lipids in archaea and evolutionary considerations. Microbiol. Mol. Biol. Rev. *71*, 97–120.

Lee, P.C., Petri, R., Mijts, B.N., Watts, K.T., and Schmidt-Dannert, C. (2005). Directed evolution of Escherichia coli farnesyl diphosphate synthase (IspA) reveals novel structural determinants of chain length specificity. Metab. Eng. *7*, 18–26.

Liang, G., Chen, D., Bastian, M., and Sigel, H. (1992). Metal ion binding properties of dihydroxyacetone phosphate and glycerol 1 -phosphate. J. Am. Chem. Soc. *114*, 7780–7785.

Lolkema, J.S., and Slotboom, D.J. (1998a). Hydropathy profile alignment: a tool to search for structural homologues of membrane proteins. FEMS Microbiol. Rev. *22*, 305–322.

Lolkema, J.S., and Slotboom, D.J. (1998b). Estimation of structural similarity of membrane proteins by hydropathy profile alignment. Mol. Membr. Biol. *15*, 33–42.

Lombard, J., López-García, P., and Moreira, D. (2012a). The early evolution of lipid membranes and the three domains of life. Nat. Rev. Microbiol. *10*, 507–515.

Lombard, J., López-García, P., and Moreira, D. (2012b). Phylogenomic investigation of phospholipid synthesis in archaea. Archaea *2012*, 630910.

Lorenzen, W., Ahrendt, T., Bozhüyük, K.A.J., and Bode, H.B. (2014). A multifunctional enzyme is involved in bacterial ether lipid biosynthesis. Nat. Chem. Biol. *10*, 425–427.

Martin, D., Gannoun-Zaki, L., Bonnefoy, S., Eldin, P., Wengelnik, K., and Vial, H. (2000). Characterization of Plasmodium falciparum CDP-diacylglycerol synthase, a proteolytically cleaved enzyme. Mol. Biochem. Parasitol. *110*, 93–105.

Matsumi, R., Atomi, H., Driessen, A.J.M., and van der Oost, J. (2011). Isoprenoid biosynthesis in Archaea—biochemical and evolutionary implications. Res. Microbiol. *162*, 39–52.

Morii, H., Nishihara, M., and Koga, Y. (2000). CTP:2,3-di-O-geranylgeranyl-sn-glycero-1-phosphate cytidyltransferase in the methanogenic archaeon Methanothermobacter thermoautotrophicus. J. Biol. Chem. *275*, 36568–36574.

Morii, H., and Koga, Y. (2003). CDP-2,3-Di-O-geranylgeranyl-sn-glycerol:L-serine O-archaetidyltransferase (archaetidylserine synthase) in the methanogenic archaeon Methanothermobacter thermautotrophicus. J. Bacteriol. *185*, 1181–1189.

Nemoto, N., Oshima, T., and Yamagishi, A. (2003). Purification and characterization of geranylgeranylglyceryl phosphate synthase from a thermoacidophilic archaeon, Thermoplasma acidophilum. J. Biochem. *133*, 651–657.

Nishihara, M., and Koga, Y. (1997). Purification and properties of sn-glycerol-1-phosphate dehydrogenase from Methanobacterium thermoautotrophicum: characterization of the biosynthetic enzyme for the enantiomeric glycerophosphate backbone of ether polar lipids of Archaea. J. Biochem. *122*, 572–576.

Nowicka, B., and Kruk, J. (2010). Occurrence, biosynthesis and function of isoprenoid quinones. Biochim. Biophys. Acta - Bioenerg. *1797*, 1587–1605.

Payandeh, J., Fujihashi, M., Gillon, W., and Pai, E.F. (2006). The crystal structure of (S)-3-O-geranylgeranylglyceryl phosphate synthase reveals an ancient fold for an ancient enzyme. J. Biol. Chem. *281*, 6070–6078.

Peterhoff, D., Beer, B., Rajendran, C., Kumpula, E.-P., Kapetaniou, E., Guldan, H., Wierenga, R.K., Sterner, R., and Babinger, P. (2014). A comprehensive analysis of the geranylgeranylglyceryl phosphate synthase enzyme family identifies novel members and reveals mechanisms of substrate specificity and quaternary structure organization. Mol. Microbiol. *92*, 885–899.

Podar, M., Makarova, K.S., Graham, D.E., Wolf, Y.I., Koonin, E.V., and Reysenbach, A.-L. (2013). Insights into archaeal evolution and symbiosis from the genomes of a nanoarchaeon and its inferred crenarchaeal host from Obsidian Pool, Yellowstone National Park. Biol. Direct *8*, 9.

Salis, H.M., Mirsky, E.A., and Voigt, C.A. (2009). Automated design of synthetic ribosome binding sites to control protein expression. Nat. Biotechnol. *27*, 946–950.

Sasaki, D., Fujihashi, M., Iwata, Y., Murakami, M., Yoshimura, T., Hemmi, H., and Miki, K. (2011). Structure and mutation analysis of archaeal geranylgeranyl reductase. J. Mol. Biol. *409*, 543–557.

Shastri, S., Zeeman, A.-M., Berry, L., Verburgh, R.J., Braun-Breton, C., Thomas, A.W., Gannoun-Zaki, L., Kocken, C.H.M., and Vial, H.J. (2010). Plasmodium CDP-DAG synthase: an atypical gene with an essential N-terminal extension. Int. J. Parasitol. *40*, 1257–1268.

Shen, H., Heacock, P.N., Clancey, C.J., and Dowhan, W. (1996). The CDS1 gene encoding CDP-diacylglycerol synthase in Saccharomyces cerevisiae is essential for cell growth. J. Biol. Chem. *271*, 789–795.

Soderberg, T., Chen, A., and Poulter, C.D. (2001). Geranylgeranylglyceryl phosphate synthase. Characterization of the recombinant enzyme from Methanobacterium thermoautotrophicum. Biochemistry *40*, 14847–14854.

Sparrow, C.P., Raetz, C.R., Shimkata, T., and Stumpf, P.K. (1985). Purification and properties of the membrane-bound CDP-diglyceride synthetase from Escherichia coli. J. Biol. Chem. *260*, 12084–12091.

Tachibana, A., Tanaka, T., Taniguchi, M., and Oi, S. (1993). Potassium-stimulating mechanism of geranylgeranyl diphosphate synthase of Methanobacterium thermoformicicum SF-4. J. Biochem. *114*, 389–392.

Tachibana, A., Yano, Y., Otani, S., Nomura, N., Sako, Y., and Taniguchi, M. (2000). Novel prenyltransferase gene encoding farnesylgeranyl diphosphate synthase from a hyperthermophilic archaeon, Aeropyrum pernix. Molecularevolution with alteration in product specificity. Eur. J. Biochem. *267*, 321–328.

van de Vossenberg, J.L., Driessen, A.J., and Konings, W.N. (1998). The essence of being extremophilic: the role of the unique archaeal membrane lipids. Extremophiles *2*, 163–170.

Villanueva, L., Damsté, J.S.S., and Schouten, S. (2014). A re-evaluation of the archaeal membrane lipid biosynthetic pathway. Nat. Rev. Microbiol. *12*, 438–448.

Wang, K., and Ohnuma, S. (1999). Chain-length determination mechanism of isoprenyl diphosphate synthases and implications for molecular evolution. Trends Biochem. Sci. *24*, 445–451.

Watanabe, Y., Nakamura, T., and Mitsumoto, H. (1997). Protection of phosphate with the 9-fluorenylmethyl group. Synthesis of unsaturated-acyl phosphatidylinositol 4,5-bisphosphate. Tetrahedron Lett. *38*, 7407–7410.

Wu, L., Niemeyer, B., Colley, N., Socolich, M., and Zuker, C.S. (1995). Regulation of PLC-mediated signalling in vivo by CDP-diacylglycerol synthase. Nature *373*, 216–222.

Wycuff, D.R., and Matthews, K.S. (2000). Generation of an AraC-araBAD promoter-regulated T7 expression system. Anal. Biochem. *277*, 67–73.

Zhang, H., Shibuya, K., Hemmi, H., Nishino, T., and Prestwich, G.D. (2006). Total synthesis of geranylgeranylglyceryl phosphate enantiomers: substrates for characterization of 2,3-O-digeranylgeranylglyceryl phosphate synthase. Org. Lett. *8*, 943–946.